Superresolution Reconstruction of Magnetic Resonance Images Based on a Nonlocal Graph Network

Yuanhang Li, Xiang Li, Yidan Yan and Chaochao Hu[*]

College of Computer Science and Technology, Henan Polytechnic University, Jiaozuo, Henan 454000, P R China

Abstract

INTRODUCTION: High-resolution (HR) medical images are very important for doctors when diagnosing the internal pathological structures of patients and formulating precise treatment plans.

OBJECTIVES: Other methods of superresolution cannot adequately capture nonlocal self-similarity information of images. To solve this problem, we proposed using graph convolution to capture non-local self-similar information.

METHODS: This paper proposed a nonlocal graph network (NLGN) to perform single magnetic resonance (MR) image SR. Specifically, the proposed network comprises a nonlocal graph module (NLGM) and a nonlocal graph attention block (NLGAB). The NLGM is designed with densely connected residual blocks, which can fully explore the features of input images and prevent the loss of information. The NLGAB is presented to efficiently capture the dependency relationships among the given data by merging a nonlocal operation (NL) and a graph attention layer (GAL). In addition, to enable the current node to aggregate more beneficial information, when information is aggregated, we aggregate the neighbor nodes that are closest to the current node.

RESULTS: For the scale r=2, the proposed NLGN achieves PSNR of 38.54 dB and SSIM of 0.9818 on the $T(T1, BD)$ dataset, and yielding a 0.27 dB and 0.0008 improvement over the CSN method, respectively.

CONCLUSION: The experimental results obtained on the IXI dataset show that the proposed NLGN performs better than the state-of-the-art methods.

[*]Corresponding author. Email: chaos-hu@home.hpu.edu.cn

1. Introduction

In recent years, medical imaging technologies, such as computed tomography (CT), magnetic resonance imaging (MRI), and positron emission tomography (PET), have played important roles in scientific research and clinical medicine. Notably, because magnetic resonance (MR) images have the advantage of producing clear images with high soft tissue contrast and distinct characteristics, they have gradually be-come the main data source for model training in medical auxiliary systems based on deep learning.

Resolution is one of the most important measures for MR images, and high-resolution (HR) MR images are especially helpful for clinicians when performing diagnoses. However, the acquisition of HR MR images may increase the cost of the system, increase the scanning time, and reduce the signal-to-noise ratio (SNR) due to the employed hardware device, body motion, and imaging time. To address these problems, superresolution (SR) reconstruction technology can be used to reconstruct low-resolution (LR) MR images, and higher-quality MR images can be obtained under the same imaging environment and hardware equipment. Image superresolution (SR) reconstruction refers to the process of recovering high-resolution (HR) images from low-resolution (LR) images. Currently, the SR reconstruction technique is

widely used for images in many fields, such as face images [1, 2], remote sensing images [4, 5], medical images [5-8].

Traditional SR methods are mainly based on interpolation [9], reconstruction [10, 11], and shallow learning [12, 13]. Although interpolation-based methods are computationally simple and efficient in terms of image details, they often lead to artifacts in reconstructed MR images. Reconstruction-based methods can overcome the unfavorable oversmoothing effects of interpolation-based methods. However, they depend on accurate image registration. Methods based on shallow learning can achieve high-quality reconstructed images. However, these methods have difficulty obtaining the optimal model parameters, and they are not suitable for most image reconstruction tasks.

With the successful application of deep learning technology in image classification [14-19], target detection [20-22], and image segmentation [23, 24], this approach has also been applied in SR reconstruction tasks. The superresolution convolutional neural network (SRCNN) [25] was first proposed based on a CNN, and it has achieved better results than those of the traditional methods. The SR approach for very deep convolutional networks (VDSR) [26] was presented to increase network depth and reduce the training difficulty based on the residual connections of a residual network (ResNet) [27]. Lim et al. [28] built a more profound and better-performing network, the enhanced deep superresolution network (EDSR), by deleting the batch normalization (BN) layer of the residual block because they found that the BN layer was not adequate for reconstruction tasks. To improve information flow, the cascaded multiscale cross network (CMSCN) [29] was proposed and used to progressively cascade a series of subnetworks together to infer high-resolution features. The channel splitting network (CSN) [6] was presented and used to divide the features into two parts along the channel dimension and adopt different mechanisms to explore different information, thus realizing the different treatment of channel features. In addition, some other improved methods were introduced by increasing the depth of the base model or reusing the derived features to achieve improved reconstruction effectiveness; such networks include the deep recursive residual network (DRRN) [30], residual dense network (RDN) [31] and the wide residual network with a fixed skip connection (FSCWRN) [7]. However, in the methods mentioned above, the spatial features are treated equally, and the dependencies among the pixels are not considered.

To fuse the dependencies among the pixels of an input image, more methods have been proposed by researchers. The nonlocal recurrent network (NLRN) [32] was proposed to capture the available nonlocal self-similarity information by the combination of a nonlocal (NL) operation module and a CNN. The residual nonlocal attention network (RNAN) [33] was proposed to improve the ability of models to capture local features via residual local and nonlocal attention blocks. This approach can also maintain the dependencies between the attention feature maps of images. Subsequently, the second-order attention network (SAN) [34] was designed with a nonlocally enhanced residual group structure and NLs to capture long-distance spatial contextual information.

Although nonlocal self-similarity was studied deeply in the NLRN [32], RNAN [33] and SAN [34], local convolution cannot describe the interrelationships between blocks. That is, it may not be used to deal with non-Euclidean data. To process non-Euclidean data, researchers introduced graph neural networks (GNNs). Graph convolution based on spectrogram theory was first proposed in convolutional GNNs (ConvGNNs) [35]. To overcome the high complexity of ConvGNNs, ChebNet [36] and a graph convolutional network (GCN) [37] were developed by approximations and simplifications. The graph attention network (GAT) [38] uses an attention mechanism to capture the similarity levels of neighbor nodes relative to the current node. Graph convolution has the advantages of possessing a strong representation ability, capturing dependency relationships, and aggregating and delivering information [39, 40]. Therefore, it has also been studied in image processing tasks. To extract the correlation between features, Xu et al. [41] performed graph convolution on the features, thereby improving the SR reconstruction effect. Yan et al. [42] used GAT [38] to explore the interrelationships between different subregions in the feature map, helping to restore the texture structure and improve the reconstruction effect. However, when the above graph convolution model aggregates information, the current node aggregates the information of all neighboring nodes, and the aggregated information may interfere with itself.

The current methods have the following shortcomings: (i) Nonlocal self-similarity information cannot be fully captured by local convolution; (ii) Most graph convolution operation may aggregate negative information to the current node. In view of the above problems, a nonlocal graph attention layer (NLGAL) is presented in this paper. It can fully capture the nonlocal self-similarity information of images by combining a GAL [38] and nonlocal self-similarity. Furthermore, a nonlocal graph network (NLGN) is designed based on the NLGAL for MR image reconstruction. The new model can capture the nonlocal self-similarity information and the remote dependencies between the obtained feature maps. Hence, it efficiently improves the quality of SR reconstruction. In addition, unfavorable information is avoided when the current node aggregates information. In this study, a new strategy is used. When information is aggregated, the top k neighbor nodes that are most similar to the current node are selected for aggregation. The IXI dataset[2] is chosen for verification and comparison with state-of-the-art methods, such as bicubic [9], the SRCNN [25], the VDSR [26], the RDN [31], CMSCN [29], the FSCWRN [7] and CSN [6]. The experimental results prove that the presented method achieves better reconstruction results than competing approaches.

The rest of this paper is organized as follows. In Section 2, we briefly review the related work. Section 3 and Section

---

[2] http://brain-development.org/ixi-dataset/

4 present a detailed analysis of the newly proposed schemes, followed by an extensive experimental comparison on the
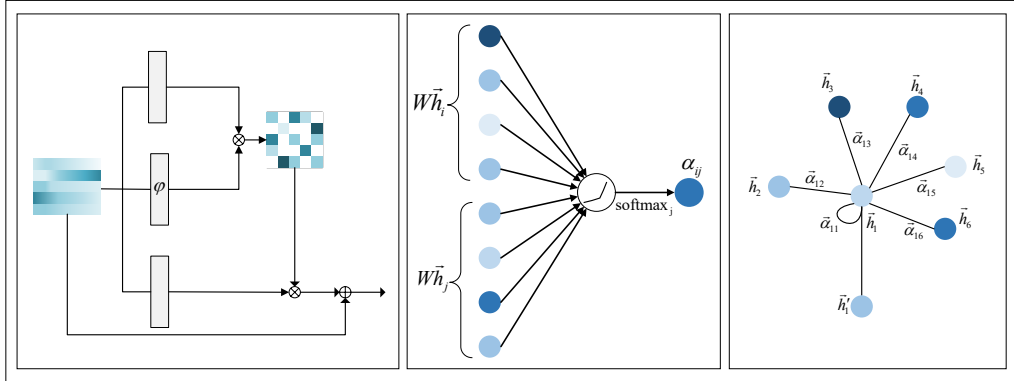
IXI dataset. Finally, we conclude our work.

Figure 1. a) Nonlocal operation (NL), b) Schematic diagram of the graph attention layer (GAL) attention weight calculation, and c) The GAL information aggregation diagram

2. Related Work

2.1. Nonlocal Operation (NL)

The nonlocal operation was proposed in the NLRN [32], and it was formulated as follows:

$$Z = \frac{1}{\delta}\sum \Phi(X)G(X) \qquad (1)$$

Where $X \in R^{N \times m}$ is the input of the NL, $Z \in R^{N \times k}$ is its output, N denotes the number of image pixels, and m and k are the input feature length and the output feature length, respectively. $\Phi(X) \in R^{N \times N}$ is a nonlocal correlation matrix, and it is used to calculate the similarity relationship between the blocks. $G(X) \in R^{N \times k}$ is a nonlocal transformation matrix. The output is normalized by $1/\delta$ with a normalization factor of δ.

As shown in Figure 1.a, the NL is implemented using a 1×1 convolution kernel, where θ, φ and g are the weight parameters, $\otimes$ represents matrix multiplication and $\oplus$ represents elementwise addition.

2.1. Graph Attention Layer (GAL)

For a set of input nodes, the GAL first calculates the attention coefficient between two nodes. For a node i and its neighbor node j, the attention coefficient e_{ij} between them is defined as follows [38]:

$$e_{ij} = a\left(W\vec{h}_i, W\vec{h}_j\right) \qquad (2)$$

Where a denotes the attention mechanism, $\vec{h}_i$ and $\vec{h}_j$ represent the feature vectors of nodes i and j, respectively, and W represents the linear transformation matrix.

Suppose that N_i represents all the neighbors of node i. To make the similarities of different nodes comparable, the *Softmax* function is used for normalization; this function is given as:

$$\alpha_{ij} = softmax(e_{ij}) = \frac{exp(e_{ij})}{\sum_{k \in N_i} exp(e_{ik})} \qquad (3)$$

The attention mechanism a is a single-layer feedforward neural network. It is parameterized by a weight vector and the leaky rectified linear unit ($LeakyReLU$) function for nonlinear activation. The calculation of the attention mechanism is shown in Figure 1.b. Therefore, α_{ij} can be further expressed as follows:

$$\alpha_{ij} = \frac{exp(LeakyReLU(\vec{a}^T[W\vec{h}_i \| W\vec{h}_j]))}{\sum_{k \in N_i} exp(LeakyReLU(\vec{a}^T[W\vec{h}_i \| W\vec{h}_k]))} \qquad (4)$$

Where T represents the transposition operation and $\|$ is the concatenation operation.

Then, $\vec{h}_i$ can be calculated by the following formula:

$$\vec{h}_i = \sigma(\sum_{j \in N_i} \alpha_{ij} W\vec{h}_j) \qquad (5)$$

where $\sigma(\cdot)$ stands for the nonlinear activation function. The information aggregation process is shown in Figure 1.c.

3. Nonlocal Graph Network (NLGN)

3.1. Network Architecture

The NLGN model proposed in the paper is shown in Figure 2.a. Similar to other image SR models, the NLGN mainly consists of three parts: a feature extraction network, a nonlinear mapping network, and a reconstruction network. The feature extraction network is used to extract the shallow features of the input image X. The deep features and

nonlocal self-similarity information are extracted and fused by the nonlinear mapping network. Finally, SR images are reconstructed by the reconstruction network.
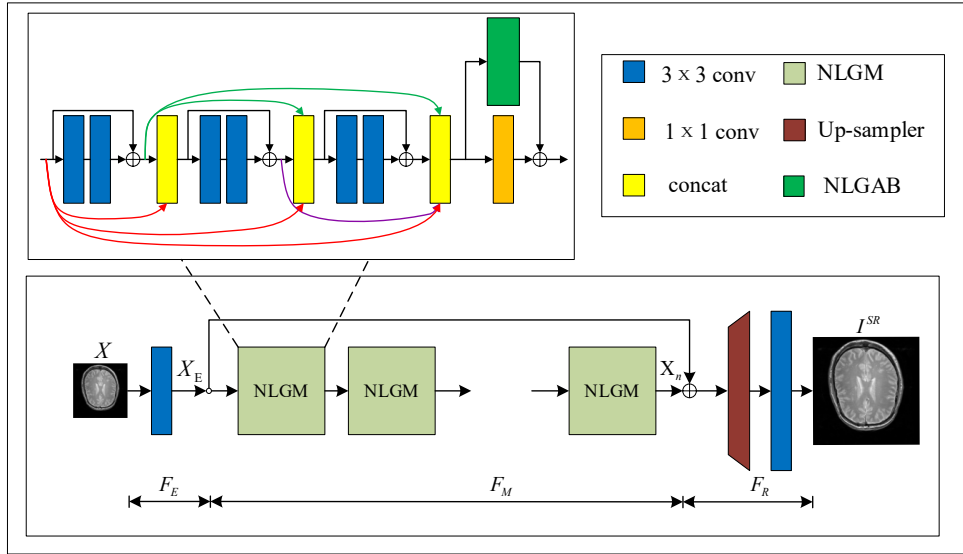

Figure 2. The diagram of the proposed NLGN. a) The overall structure. b) The architecture of the nonlocal graph module

Feature Extraction Network

The feature extraction network only uses a 3×3 convolution to extract the input shallow features. $F_E(\cdot)$ denotes the mapping function of the network, and the extracted feature X_E can be represented as:

$$X_E = F_E(X) \tag{6}$$

Where X represents a low-resolution input image.

Nonlinear Mapping Network

The nonlinear mapping network contains a series of stacked nonlocal graph modules (NLGMs). X_E represents the input of the first NLGM. And the input and output of the i-th NLGM are X_{i-1} and X_i, respectively. Therefore, the output X_i of the i-th NLGM can be expressed as:

$$X_i = F_{nlgm}^i(X_{i-1}), i = 1, \cdots, n, \tag{7}$$

Where $F_{nlgm}^i(\cdot)$ corresponds to the operations of the i-th NLGM. For convenience, $X_E = X_0$. Then, the output of the last network, which is the output of the nonlinear mapping network, can be expressed as:

$$\begin{aligned} X_n &= F_M(X_E) \\ &= F_{nlgm}^n(X_{n-1}) = F_{nlgm}^n(F_{nlgm}^{n-1}(\cdots(F_{nlgm}^1(X_0))\cdots)) \end{aligned} \tag{8}$$

Where X_n represents the output of the n-th NLGM, X_{n-1} represents the input of the n-th NLGM, and similarly, X_0 represents the input of the first NLGM. $F_M(\cdot)$ denotes the mapping function of the nonlinear mapping network.

Reconstruction Network

The reconstruction network consists of an upsampling module and a 3×3 convolutional layer. The upsampling module first reconstructs the input feature maps into SR features through a subpixel shuffling layer [43]. Then, the network uses a 3×3 convolutional layer to build the SR features into the final output. The mapping function of the reconstruction network can be expressed as follows:

$$I^{SR} = F_R(X_n + X_E) \tag{9}$$

Where X_n and X_E represent the deep and shallow features of the input images respectively, I^{SR} represents the output, $F_R(\cdot)$ represents the mapping function of the reconstruction network.

3.2. Nonlocal Graph Module

The architecture of the NLGM is shown in Figure 2.b. It is composed of a dense residual block [44] and a nonlocal graph attention block (NLGAB).

Dense Residual Block

The dense residual block is composed of three densely connected residual blocks, and each residual block has two convolutional layers and two *ReLU* activation functions. The output X_{DR} of the dense residual block can be expressed as:

$$X_{DR} = F_{DR}(X_{i-1}) \tag{10}$$

Where X_{i-1} represents the input of the i-th NLGM and $F_{DR}(\cdot)$ represents the mapping function of the dense residual block. Dense residual blocks can prevent the loss of

information during feature transfer. For more information, please refer to [44].

NLGAB

The NLGAB architecture is shown in Figure 3. It is mainly composed of an NLGAL and convolutions. The NLGAB first uses a 1×1 convolutional layer to reduce the dimensionality of X_{DR}. Then, it chooses a 3×3 convolutional layer with a stride of 2 for downsampling, and the downsampled features are used as the inputs of the proposed NLGAL. After that, deconvolution is introduced to restore the generated output to its original size. Finally, a 1×1 convolutional layer is applied to compress and reconstruct the deconvolution result. The whole procedure can be expressed as follows:

$$X_{NLGAB} = F_{NLGAB}(X_{DR})$$
$$= f_{c\_1\times1}(f_{dc\_3\times3}(F_{NLGAL}(f_{c\_3\times3,s=2}(f_{c\_1\times1}(X_{DR})))))$$ (11)

Where $F_{NLGAB}(\cdot)$ represents the mapping function of the NLGAB, $f_{c\_1\times1}(\cdot)$ is a 1×1 convolution, $f_{dc\_3\times3}(\cdot)$ is a 3×3 deconvolution, $F_{NLGAL}(\cdot)$ represents the NLGAL, and $f_{c\_3\times3,s=2}(\cdot)$ is a 3×3 convolution with a stride of 2.
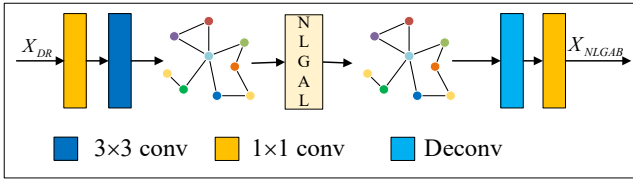

Figure 3. Nonlocal graph attention block (NLGAB)

Generally, for an NLGM, the dense residual block is first used to deal with the input information. Then, the NLGAB is presented to capture the nonlocal self-similarity information of X_{DR}. In addition, X_{DR} is further processed by the bottleneck layer for compression. Finally, the output of the NLGAB and the compression result are combined as

the input of the next NLGM. Furthermore, the output of an NLGM can be expressed as:

$$X_i = F_{NLGM}(X_{i-1}) = f_{c\_1\times1}(X_{DR}) + F_{NLGAB}(X_{DR})$$ (12)

Where X_i is the output of the i-th NLGM, $f_{c\_1\times1}(\cdot)$ is the bottleneck layer with 1×1 convolution, and $F_{NLGAB}(\cdot)$ represents the operation of NLGAB.

3.3. Nonlocal Graph Attention Layer (NLGAL)

Both the GAL [38] and NLs [32] can capture the context information and remote dependencies. However, they are different from each other. NLs are used to aggregate the information between all blocks. However, only the information between the neighboring nodes in each block is aggregated by the GAL. In addition, NLs cannot fully capture the relationship between two blocks by convolution. The GAL can effectively characterize and calculate the relationship between two blocks (that is, the adjacent nodes). In general, the GAL is more suitable for capturing nonlocal information than NLs. However, the space and time complexity of the GAL is very large due to the use of a parameter matrix and a single-layer feedforward neural network.

By the combination of NLs and the GAL, the NLGAL is proposed in this paper. Specifically, a linearly embedded Gaussian kernel is chosen to replace the calculation of the attention coefficient in the GAL. In addition, convolution is used to realize the linear transformation. Formula (4) is rewritten as:

$$\alpha_{ij} = \frac{exp(LeakyReLU((W\vec{h}_i W_\theta)(W\vec{h}_j W_\varphi)^T))}{\sum_{k\in N_i} exp(LeakyReLU((W\vec{h}_i W_\theta)(W\vec{h}_k W_\varphi)^T))}$$ (13)

Where W, W_θ and $W\varphi$ are learnable parameters. And we used Formula (13) to calculate the similarity between nodes (that is attention coefficient). The operation of the NLGAL is shown in Figure 4.
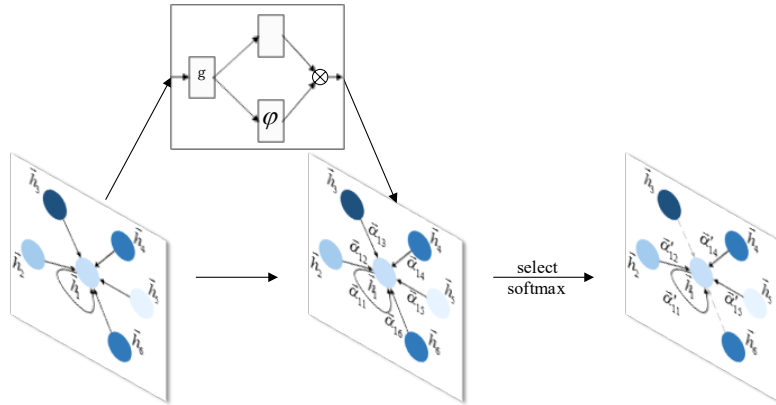

Figure 4. The architecture of the nonlocal graph attention layer

[10] Medoff, B.P., Brody, W.R., Nassi, M. and Macovski, A. Iterative convolution backprojection algorithms for image reconstruction from limited data. J. Opt. Soc. Am. 1983; 73(11): 1493–1500.

[11] Stark, H. and Oskoui, P. High-resolution image recovery from image-plane arrays, using convex projections. J. Opt. Soc. Am. A. 1989; 6(11): 1715–1726.

[12] Yang, J., Wright, J., Huang, T.S. and Ma, Y. Image super-resolution via sparse representation. IEEE Transactions on Image Processing. 2010; 19(11): 2861–2873.

[13] Zhu, Q. Image superresolution via sparse embedding. In Amir, A. Proceedings. Proceeding of the 11th World Congress on Intelligent Control and Automation; 29 June-4 July 2014; Shengyang, China. Piscataway, NJ: IEEE; 2014. 5673–5676.

[14] Yang, L., Wang, S.H. and Zhang, Y.D. (2022) Ednc: Ensemble deep neural network for covid-19 recognition. Tomography. 2020; 8(2): 869–890.

[15] Zhou, Q., Zhang, X. and Zhang, Y.D. Ensemble learning with attention-based multiple instance pooling for classification of spt. IEEE Transactions on Circuits and Systems II: Express Briefs. 2022; 69(3): 1927–1931.

[16] Zhang, Y.D., Satapathy, S.C. and Wang, S.H. (2022) Fruit category classification by fractional fourier entropy with rotation angle vector grid and stacked sparse autoencoder. Expert Systems. 2022; 39(3), Article: e12701.

[17] Wang, S.H., Satapathy, S.C., Zhou, Q., Zhang, X. and Zhang, Y.D. Secondary pulmonary tuberculosis identification via pseudo-zernike moment and deep stacked sparse autoencoder. Journal of Grid Computing. 2022; 20(1): 1–16.

[18] Shui-Hua, W., Khan, M.A., Govindaraj, V., Fernandes, S.L., Zhu, Z. and Yu-Dong, Z. Deep rankbased average pooling network for covid-19 recognition. Computers, Materials, & Continua. 2022; 70(2): 2797–2813.

[19] Shui-Hua Wang, Muhammad Attique Khan, Y.D.Z. Vispnn: Vgg-inspired stochastic pooling neural network. Computers, Materials & Continua. 2022; 70(2): 3081–3097.

[20] Redmon, J. Yolo9000: better, faster, stronger. In G. L. Proceedings. Proceedings of the IEEE conference on computer vision and pattern recognition; July 21-26 2017; Honolulu, HI, USA. Piscataway, NJ: IEEE; 2017. pp. 7263–7271.

[21] Bochkovskiy, A., Wang, C.Y. and Liao, H.Y.M. Yolov4: Optimal speed and accuracy of object detection. arXiv preprint arXiv: 2004.10934, 2020.

[22] Lin, T.Y. Feature pyramid networks for object detection. In G. L. Proceedings. Proceedings of the IEEE conference on computer vision and pattern recognition; July 21-26 2017; Honolulu, HI, USA. Piscataway, NJ: IEEE; 2017. pp. 936–944.

[23] Long, J. Fully convolutional networks for semantic segmentation. In Los Alamitos. Proceedings. Proceedings of 2015 IEEE Conference on Computer Vision and Pattern Recognition; June 7-15 2015; Boston, MA, USA. Piscataway, NJ: IEEE; 2015. pp. 3431–3440.

[24] Ronneberger, O., Fischer, P. and Brox, T. U-net: Convolutional networks for biomedical image segmentation. arXiv preprint arXiv:1505.04597, 2015.

[25] Dong, C. Learning a deep convolutional network for image superresolution. In Fleet, D. Proceedings. Proceedings of the 2014 European Conference on Computer Vision; Sep 6-12, 2014; Zurich, Switzerland.2014 Cham: Springer International Publishing; 2014, pp. 184–199.

[26] Kim, J., Lee, J.K. and Lee, K.M. Accurate image super-resolution using very deep convolutional networks. arXiv preprint arXiv: 1511.04587, 2015.

[27] He, K. Deep residual learning for image recognition. In R. B. Proceedings. Proceedings of the IEEE conference on computer vision and pattern recognition; June 27-30, 2016; Las Vegas, NV, USA. Piscataway, NJ: IEEE; 2016. pp. 770–778.

[28] Lim, B., Son, S., Kim, H., Nah, S. and Lee, K.M. (2017), Enhanced deep residual networks for single image super-resolution. arXiv preprint arXiv: 1707.02921, 2017.

[29] Hu, Y., Gao, X., Li, J., Huang, Y. and Wang, H. Single image super-resolution with multi-scale information cross-fusion network. Signal Processing. 2021; 179: 107831.

[30] Tai, Y. Image superresolution via deep recursive residual network. In G. L. Proceedings of the IEEE conference on computer vision and pattern recognition; July 21-26 2017; Honolulu, HI, USA. Piscataway, NJ: IEEE; 2017. pp. 2790–2798.

[31] Zhang, Y. Residual dense network for image super-resolution. In Brown. M. Proceedings. the IEEE conference on computer vision and pattern recognition; Jun 18-22 2018, Salt Lake City, Utah, USA. Piscataway, NJ: IEEE; 2019. pp. 2472–2481.

[32] Liu D, Wen B, Fan Y, et al. Non-local recurrent network for image restoration. Advances in neural information processing systems, 2018, 31: 1680–1689.

[33] Zhang, Y., Li, K., Li, K., Zhong, B. and Fu, Y. Residual non-local attention networks for image restoration. arXiv preprint arXiv: 1903.10082, 2019

[34] Dai, T. Second-order attention network for single image superresolution. In Davis L. Proceedings. Proceedings of the IEEE conference on Computer Vision and Pattern Recognition; Jun 16-20, 2019; Long Beach, CA, USA. Piscataway, NJ: IEEE; 2019. pp. 11057–11066.

[35] Bruna J, Zaremba W, Szlam A, et al. Spectral networks and locally connected networks on graphs[J]. arXiv preprint arXiv:1312.6203, 2013.

[36] Defferrard, M., Bresson, X. and Vandergheynst, P. Convolutional neural networks on graphs with fast localized spectral filtering. Advances in neural information processing systems, 2016, 29: 3844–3852.

[37] Kipf, T.N. and Welling, M. Semi-supervised classification with graph convolutional networks. arXiv preprint arXiv: 1609. 02907, 2019.

[38] Veli ˇ ckovi ´ c, P., Cucurull, G., Casanova, A., Romero, A., Lio˙, P. and Bengio, Y. Graph attention networks. arXiv preprint arXiv: 1710.10903, 2017.

[39] Wu, Z., Pan, S., Chen, F., Long, G., Zhang, C. and Yu, P.S. A comprehensive survey on graph neural networks. IEEE Transactions on Neural Networks and Learning Systems. 2021; 32(1): 4–24.

[40] Chami, I., Abu-El-Haija, S., Perozzi, B., Ré, C. and Murphy, K. (2021), Machine learning on graphs: A model and comprehensive taxonomy. arXiv preprint arXiv: 2005.03675, 2020.

[41] Xu, B. and Yin, H. Graph convolutional networks in feature space for image deblurring and super-resolution. arXiv preprint arXiv: 2105.10465, 2105.

[42] Yan, Y., Ren, W., Hu, X., Li, K., Shen, H. and Cao, X. SRGAT: Single image super-resolution with graph attention network. IEEE Transactions on Image Processing. 2021; 30: 4905–4918.

[43] Shi, W., Caballero, J., Huszár, F., Totz, J., Aitken, A.P., Bishop, R., Rueckert, D. et al. Real-time single image and video super-resolution using an efficient subpixel

12

convolutional neural network. arXiv preprint arXiv: 1609.05158, 2016.

[44] Anwar, S. and Barnes, N. Densely residual laplacian super-resolution. IEEE Transactions on Pattern Analysis and Machine Intelligence. 2022; 44(3): 1192–11204.

[45] Wang, Z., Bovik, A., Sheikh, H. and Simoncelli, E. Image quality assessment: from error visibility to structural similarity. IEEE Transactions on Image Processing. 2004; 13(4): 600–612.